

O K-edge x-ray absorption study of ultrathin NiO epilayers deposited *in situ* on Ag(001)

E. Groppo, C. Prestipino, and C. Lamberti*

Department of Inorganic, Physical and Materials Chemistry, and NIS centre of excellence, University of Torino, Via P. Giuria 7, I-10125 Torino Italy and INFN - U.d.R. di Torino

R. Carboni and F. Boscherini

INFN and Dipartimento di Fisica, Università di Bologna, Viale C. Berti Pichat 6/2, I-40127 Bologna, Italy

P. Luches, S. Valeri, and S. D'Addato

INFN- National Center on nanoStructures and bioSystems at Surfaces (S³) and Dipartimento di Fisica, Università di Modena e Reggio Emilia, Via G. Campi 213/a, I-41100 Modena, Italy

(Received 9 January 2004; revised manuscript received 25 June 2004; published 14 October 2004)

In a recent contribution [Phys. Rev. Lett. **91**, 046101 (2003)] we used polarization-dependent, Ni *K* edge, x-ray absorption spectroscopy (XAS) to probe the structure of ultrathin NiO epilayers deposited on Ag(001). In that experiment samples were measured *ex-situ* and a 5 ML-thick MgO cap was used to avoid the hydroxylation of the NiO film. In the present paper we report complementary O *K* edge XAS data on the same system; NiO epilayers, in the 3–50 ML thickness range, were grown *in situ* in the end station of the ALOISA beamline of the ELETTRA facility. A quantitative analysis of the data in the extended energy range has been performed using multiple scattering simulations. We found that, even in the ultrathin limit, the local structure of the film is rock-salt and we obtained a quantitative evaluation of the average in-plane and out-of-plane film strain as a function of the film thickness *T*. An in-plane compressive strain, due to lattice mismatch with the Ag substrate, is clearly present for the 3 ML film, being the in- and out-of-plane nearest neighbor distances equal to $r_{\parallel} = 2.048 \pm 0.016$ Å and $r_{\perp} = 2.116 \pm 0.018$ Å. These values are in agreement with the expected behavior for a tetragonal distortion of the unit cell. The growth-induced strain is gradually released with increasing *T*: it is still appreciable for 10 ML but is completely relaxed at 50 ML. Any significant intermixing with the Ag substrate has been ruled out. Combining O and Ni *K* edge results we can conclude that NiO films grow on Ag(001) in the O-on-Ag configuration, with an interface distance $d = 2.28 \pm 0.08$ Å. This expansion of the interplanar distance is in agreement with recent *ab initio* simulations. A comparison with the similar MgO/Ag(001) system is also performed.

DOI: 10.1103/PhysRevB.70.165408

PACS number(s): 68.55.–a, 68.35.–p, 61.10.Ht, 81.05.Je

I. INTRODUCTION

Recently, the physical properties of two-dimensional metal oxide epilayers on metal substrates have become a topic of great interest.^{1–8} Films of a few monolayers (ML) can be deposited epitaxially on metal substrates by ultra-high vacuum techniques, yielding reproducible and well-characterized systems. In this regard, note that the choice of Ag(001) as substrate for growing thin NiO and MgO layers is related to the fact that its lattice parameter $a_{\text{Ag}(001)} = 4.090$ Å is quite close to that of NiO ($a = 4.176$ Å) and of MgO ($a = 4.220$ Å), resulting in lattice strains compatible with the bidimensional growth of few ML: $\varepsilon_{\parallel} = -0.0206$ and -0.0308 for NiO and MgO, respectively.

The structure of ultrathin NiO films grown on Ag(001) has been previously studied with Auger electron diffraction,⁹ photoelectron diffraction,¹⁰ primary beam diffraction modulated electron emission (PDMEE),^{8,11} low energy electron diffraction,^{11–13} electron energy loss¹² and direct^{10,14–17} and inverse¹⁵ electron photoemission spectroscopies. The films grow in the (1 × 1) structure (where the in-plane lattice parameter of epilayer and substrate are equal), with O on top of Ag, up to a thickness of $T \sim 5$ ML. For higher coverages it has been suggested that strain is released by the introduction

of misfit dislocations.¹³ The film morphology has been investigated by means of STM,^{18,19} which suggested a rather complex interface with NiO island formation and the presence of vacancy islands in the Ag substrate after NiO deposition. Ultra thin NiO films also exhibit interesting magnetic properties^{20–23} different from the bulk.²⁴ A complete polarization-dependent XAS study, at the Ni *K* edge, has been reported by us^{8,25,26} on two NiO/Ag(001) samples with $T = 3$ and 10 ML; both samples have been capped by 5 ML of MgO to avoid surface hydroxylation. The MgO cap was chosen because of the chemical similarity with NiO and in view of the small relative misfit. Experimental results obtained in Refs. 8 and 26 are summarized in Table I, together with those obtained with *ab initio* calculations. In order to provide a complementary probe of the local structure, to investigate more directly the O-Ag interface atomic correlations and, finally, to verify whether the presence of the MgO strained cap layer ($T \sim 5$ ML) in the previous experiment significantly modifies the structure of the NiO films, in the present paper we report complementary O *K*-edge XAS experiments performed on NiO epilayers ($T = 3, 10$ and 50 ML, calibrated using x-ray reflectivity) grown *in situ* on Ag(001) in the end station of the ALOISA beamline of the ELETTRA facility (data also summarized in Table I).

TABLE I. A summary of the in- (r_{\parallel}) and out-of-plane (r_{\perp}) NiO nearest neighbor distances and of the interface distance d in the NiO/Ag(001) system, as a function of the oxide thickness T , obtained with different experimental and theoretical methods.

T (ML)	Technique	r_{\parallel} (Å)	r_{\perp} (Å)	d (Å)
Bulk	XAS Ni K edge ^a	2.092 ± 0.004	as r_{\parallel}	-
50	XAS O K edge ^c	2.082 ± 0.004	as r_{\parallel}	-
10	XAS Ni K edge ^a	2.052 ± 0.006	2.101 ± 0.006	-
10	XAS O K edge ^c	2.057 ± 0.009	2.109 ± 0.008	-
3	XAS Ni K edge ^{a,b}	2.046 ± 0.009	2.12 ± 0.02	2.37 ± 0.05
3	XAS O K edge ^c	2.048 ± 0.016	2.116 ± 0.018	2.28 ± 0.08
4	PDME ^b	-	-	2.3 ± 0.1
2	<i>ab initio</i> ^b	2.07 (fixed)	2.10	2.40

^aData from Ref. 26.

^bData from Ref. 8.

^cThis work.

II. EXPERIMENTAL AND METHODS

The samples used for the O K edge study are three NiO epilayers: 3, 10, and 50 ML thick, grown on Ag(001) single crystals *in situ*, to avoid both NiO hydroxylation and the contribution to the O signal coming from air exposure of the sample. We therefore used the tools and the procedures for NiO growth described elsewhere¹⁰ in the end station of the ALOISA beamline of the ELETTRA facility. The Ag(001) substrate was cleaned by repeated cycles of sputtering (1 keV) and annealing (720 K) in UHV. The evaporation rates were measured by means of a quartz crystal microbalance. NiO epilayers were grown using a Knudsen cell and a directional O₂ flux on the sample, resulting in a background oxygen pressure of 2×10^{-6} mbar in the growth chamber. The rate of oxide formation was approximately 1 ML/min, as evaluated by the deposition rates and the relative Ni density in metallic Ni and in NiO. The Ag substrate was kept at 460 K during the growth to enhance surface mobility.

XAS data have been acquired in the partial electron yield mode using a channeltron with 450 V retarding voltage. When performing photon energy scans in the 500–800 eV range (sampling step: 0.4 eV), to maximize the photon flux we have simultaneously scanned the undulator gap. We have been forced to choose an upper limit of 800 eV in the XAS scans, due to the presence of Ni absorption L edges. All data have been collected in grazing incidence geometry, with an incidence angle of the x-ray beam on the surface equal to 2.2°, with the electric field in or perpendicular to the (001) plane to discriminate in- and out-of-plane atomic correlations (these geometries will be termed *s* and *p* polarizations, respectively).^{8,25–29} For each sample and for each polarization a number of XAS spectra, ranging between 5 and 10, have been acquired. In order to obtain the absorption coefficient μ , the raw partial yield data have been divided by the yield data of the clean Ag surface, with both signals normalized to their I_0 , obtained measuring the drain current from the Au-coated post-focusing mirror of the beamline.³⁰ This procedure was necessary to remove some spurious effects

due to the undulator gap scanning, the presence of Cr and Fe L edges structures in our data coming from impurities in the optics, and the structured background coming from the photoabsorption cross section of Ag. The extraction of the $\chi(k)$ from the normalized spectra and their analysis using the FEFF 8.10 code³¹ has been obtained using the methods reported elsewhere,²⁶ and here only briefly recalled. The experimental $k^2\chi(k)$ data have been Fourier transformed in the 1.8–8.0 Å⁻¹ interval and then fitted in R-space in the 1.1–3.2 Å interval, thus including up to the third coordination shell around O [Fig. 1(b)]. Seven parameters have been optimized: the edge energy shift (ΔE_0), the amplitude reduction factor (S_0^2), the in- and out-of-plane first shell interatomic distances (r_{\parallel} and r_{\perp}) and the Debye-Waller factors of the first three coordination shells (σ_i , $i=1, 2, 3$). It is worth noticing that r_{\parallel} and r_{\perp} are the only two structural parameters refined in the fit. All single and multiple scattering path lengths have been derived from r_{\parallel} and r_{\perp} by simple geometrical relationships derived assuming a tetragonal cell of the epilayer. As an example, the in- and out-of-plane second shell distances are $(2r_{\parallel}^2)^{1/2}$ and $(r_{\parallel}^2 + r_{\perp}^2)^{1/2}$, respectively. The geometrical definitions of single and multiple scattering path lengths (up to the seventh coordination shell) in both *s*- and *p*- polarizations can be found in Table 3 of Ref. 26 and in Table 2 of Ref. 29, respectively. As for the 3 ML sample, measured in *p*-polarization, an additional O-Ag contribution from the Ag(001) substrate has been included in the fitting procedure to reproduce the experimental signal, as described below.

III. RESULTS AND DISCUSSION

The XPS spectra, collected *in situ* after growth [Fig. 1(c)], exhibit a bulk-like lineshape. At the three thickness investigated the spectra are dominated by the $2p_{1/2}$ and $2p_{3/2}$ peaks at binding energies (BE) of 870 eV and 852 eV, respectively. The satellite structures at 878 eV and 858 eV BE are related to $3d^8$ and $3d^{10}$ final states. The $2p_{3/2}$ peak also shows a nonlocal screening satellite at 853.5 eV.³² The BE of the main peaks and satellites and their relative intensity are clear indications that the films have a NiO bulk-like electronic structure. This is an important check on the long range scale of the sample, complementary to the local sensibility of the EXAFS technique.

Coming to the EXAFS data, the quality of the fits can be appreciated in Fig. 1(b) and the obtained structural parameters have been summarized in Table I. For each fit, the first shell Debye-Waller factor, the number of degrees of freedom (defined as the difference between the number of independent points in data and the number of variables in fit) and the FEFFIT *r*-factors,³³ lying in the 0.023–0.045 range, are reported in Table II. Due to strain relaxation, the $T=50$ ML samples behaves (within the sensitivity of XAS) as a bulk sample. In that case only 6 parameters have been optimized in the fit, as $r_{\parallel}=r_{\perp}$ (*vide supra* section II). Figure 2 summarizes the out-of-plane O-Ni distance as a function of the in-plane one (open square and triangle), along with the results from previous experiments collected at the Ni K edge^{8,26} (full square and triangle). The full star represents unstrained bulk NiO ($r_{\parallel}=r_{\perp}=r_0=2.088$ Å) as determined by XRD, while the

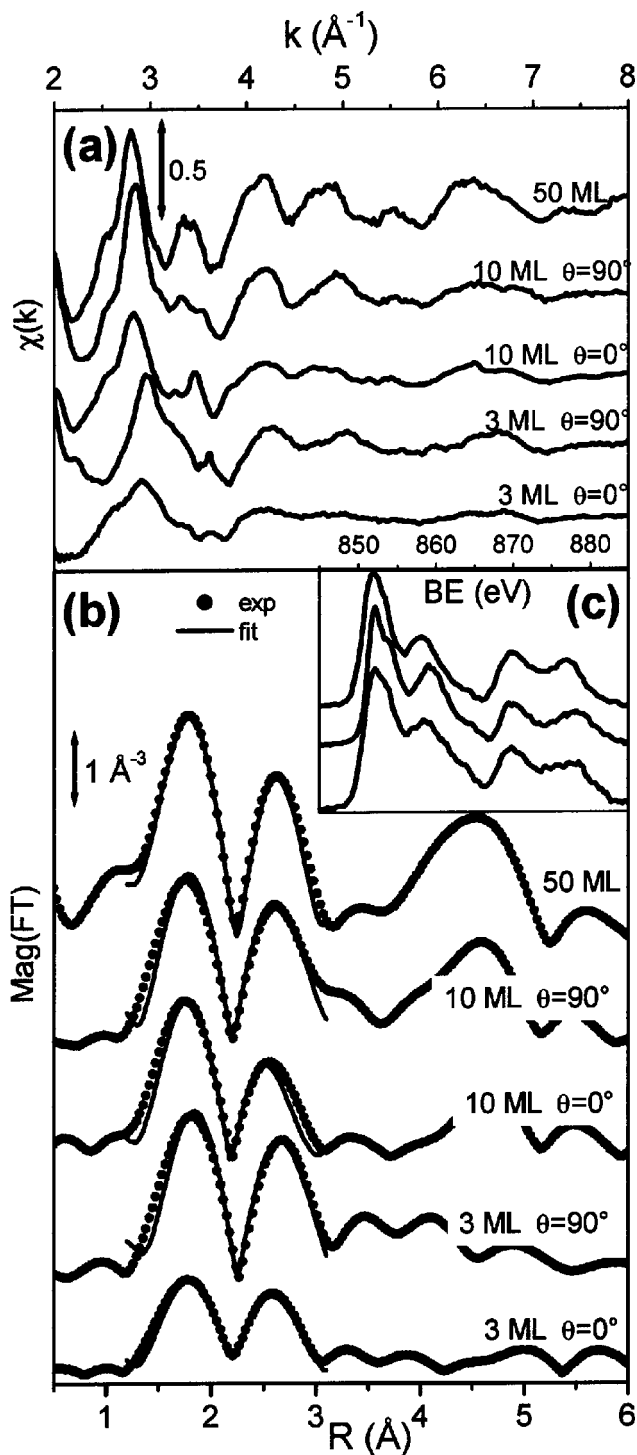


FIG. 1. (a) Raw O K edge $\chi(k)$ data of NiO/Ag(001) films as a function of both film thickness and beam polarization $s(\theta=90^\circ)$ and $p(\theta=90^\circ)$, where θ is the angle between the electric field vector and the vector normal to the (001) surface. (b) A comparison between experimental (points) and best fit (solid line) for the modulus of the k^2 -weighted, phase uncorrected FTs of the $\chi(k)$ data reported in part (a). (c) XPS spectra collected *in situ* (from top to bottom: $T=50, 10$ and 3 ML).

TABLE II. For each fit of the experimental data the table report the following: the optimized first shell Debye-Waller factor σ_1^2 ; the r factor (r factors have been defined according to Ref. 33) and the number of degrees of freedom.

Sample polarization	$\sigma_1^2(\text{\AA}^2)$	r -factor	Number of degrees of freedom in fit
50 ML	0.003 ± 0.002	0.030	4.438
10 ML/s	0.011 ± 0.004	0.045	3.234
10 ML/p	0.011 ± 0.002	0.023	3.961
3 ML/s	0.011 ± 0.003	0.034	3.102
3 ML/p (with Ag)	0.016 ± 0.007	0.028	1.434
3 ML/p (without Ag)	0.012 ± 0.004	0.112	3.434

circles (full and open for Ni and O K edges, respectively) represent the XAS value obtained from unstrained (or strain released) NiO. The straight line is obtained following the elastic theory approximation, according to the equation $r_\perp = -\gamma r_\parallel + (1 + \gamma)r_0$,²⁹ where γ is defined as $\gamma = 2C_{12}/C_{11}$, C_{11} and C_{12} being the elastic stiffness constants of bulk NiO. Values of $C_{11} = 344.6$ GPa and $C_{12} = 141$ GPa result in $\gamma = 0.818$.³⁴ The open star represents the values expected for an ideal NiO film with $r_\parallel = 1/2a_{\text{Ag}(001)} = 2.045$ \AA and consequently $r_\perp = 2.125$ \AA. The $T=10$ ML (triangles) and 3 ML (squares) positions have been represented using the r_\parallel and r_\perp values obtained from analysis of the data collected in the two different polarizations. *Ab initio* calculations performed by a CRYSTAL code on $T=2$ ML NiO film, constrained in plane by imposing perfect growth on the Ag structure ($r_\parallel = 2.07$ \AA as calculated with the same code), resulted in $r_\perp = 2.10$ \AA (open diamond in Fig. 2).⁸ On the basis of these data two main considerations can be drawn.

(i) Both 10 ML and 3 ML films are compressed in the growth plane, in order to fit the smaller Ag(001) substrate lattice constant. The 3 ML film exhibit r_\parallel and r_\perp values very similar to those expected for a perfect (1×1) growth in which the in-plane lattice parameter of epilayer and substrate are equal, while the 10 ML film appears partially relaxed along the growth direction. This suggests that the critical thickness for strain release lies between 3 and 10 ML. The in-plane contraction of the 10 ML film is in apparent disagreement with the results of other works which, on the basis of electron scattering experiments, find a critical thickness for strain release of 5 ML.^{10,13} This difference can be understood on the basis of the different sampling depth of the different techniques. In the case of XAS spectra the information comes from the whole thickness of the sample and allows us to affirm that most parts of the atoms in the 10 ML film are still in an in-plane contracted local environment. Electron scattering techniques, instead, sample only the outermost film layers, which can be in a more relaxed environment. Being the O-Ni (Ni-O) values obtained from XAS an average of the situation seen by O (Ni) atoms in all layers, the combination of our XAS results (present study and Refs. 8, 25, and 26) and the electron diffraction ones^{10,13} suggests a model where strain relaxation starts around $5-6$ ML and

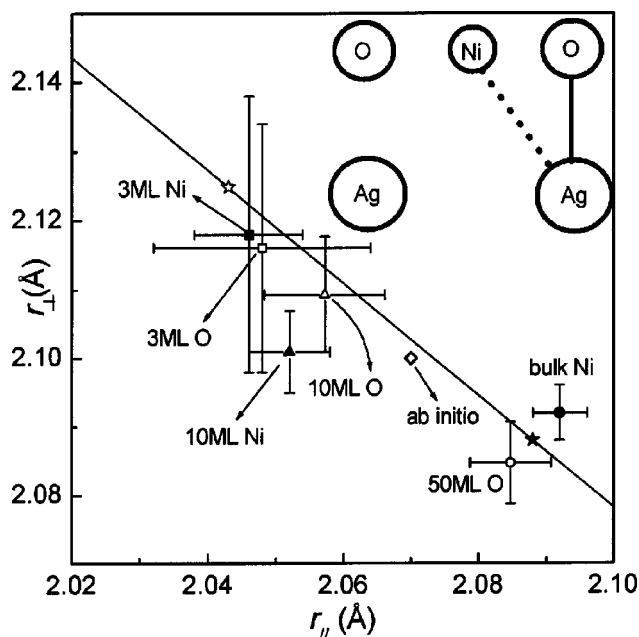


FIG. 2. Out-of-plane (r_{\perp}) and in-plane (r_{\parallel}) nearest neighbor distances obtained by the analysis of Ni (full markers) and O K edge (open markers) XAS data for the 10 (triangles) and 3 (squares) ML films and for the NiO reference samples, with the relative uncertainties. Full and open stars represent the r_{\perp} and r_{\parallel} values for unstrained NiO bulk (XRD) and for NiO perfectly epitaxial with Ag(001), respectively. The open diamond represents the value obtained by *ab initio* calculations performed on a 2 ML NiO/Ag(001) system by a CRYSTAL code. Note that the simulated NiO/Ag(001) results less strained than the experimental one owing to a theoretical half lattice parameter of Ag bulk of 2.07 Å. The solid line represents the theoretical r_{\perp} vs r_{\parallel} relationship predicted by the elastic theory, adopting the γ constant of NiO bulk.³⁴ The top right corner hosts a scheme of the Ag/NiO interface determined by combined O and Ni K edge XAS data. Full and dotted lines represent the $r_{\text{O-Ag}}=d$ (O K edge) and the $r_{\text{Ni-Ag}}$ (Ni K edge) distances, respectively.

affects only the subsequent layers, being the first 4–5 still strained.

(ii) The new O K edge data, although characterized by larger error bars (due to the smaller available k range), are in fair agreement with those obtained at the Ni K edge on MgO capped samples,^{8,25,26} for both $T=3$ and 10 ML. The same is true if the experimental result for the thinner film is compared to the *ab-initio* calculations performed on $T=2$ ML models;⁸ see Table I. This result confirms and validates our previous results^{8,25,26} and proves that the use of a few ML thick MgO capping layers are an effective mean to protect as grown NiO layers without appreciably modifying its structure. A similar result has been recently obtained by Luches *et al.* on the MgO/Ag(001) system by comparing Mg K edge data of NiO capped films to O K edge data obtained on *in-situ* grown MgO films.^{27,28}

After having described the structure of the strained NiO film itself, let us now discuss the NiO/Ag(001) interface. In the $T=3$ ML films, 1/3 of the oxide atoms (O or Ni) are interface atoms. As a consequence, the XAS signals collected on such samples with p polarization contain an appre-

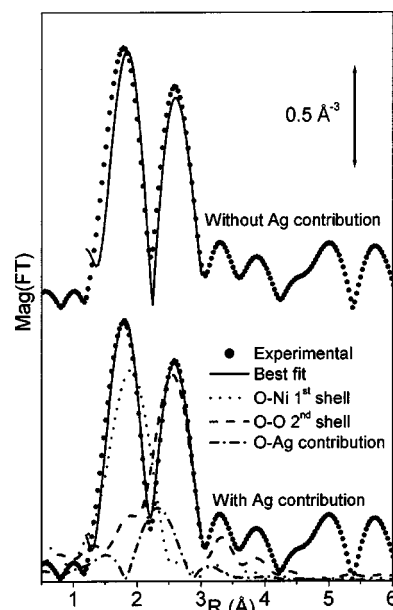


FIG. 3. A comparison between experimental (points) and best fit (solid line) for the modulus of the k^2 -weighted, phase uncorrected FTs of the experimental $\chi(k)$ of 3 ML ($\theta=0^\circ$). The upper curves refer to a fit including the signals from the tetragonally distorted NiO film only (i.e., with the same approach used in the fits of all other signals). Bottom curves refer to the fit performed by including the O-Ag signal from the Ag substrate (dashed dotted line). Also reported are the most relevant contribution to the simulated curve.

ciable O-Ag (Ni-Ag) contribution. In fact, a fit of the 3 ML in p -polarization performed considering only NiO contributions (as done in all the other cases) fails in reproducing the experimental data; see the vertically translated curves in Fig. 3. As in our previous Ni K edge study,²⁶ a much better agreement has been obtained by including a contribution from the Ag scatterers; see the bottom curves in Fig. 3; note that the corresponding r -factor moves from 0.112 to 0.028 after the inclusion of the silver contribution; see Table II. This implies two additional fitting parameters which are the O-Ag distance $r_{\text{O-Ag}}$, and its corresponding Debye-Waller factor. As for the NiO contributions the coordination number has been fixed to that expected in the case of a perfect two-dimensional layer ($N_{\text{Ag}}=1/6$). We found an O-Ag distance of $r_{\text{O-Ag}}=2.28\pm 0.08$ Å.

In the Ni K edge XAS case, a Ni-Ag signal at $r_{\text{Ni-Ag}}=3.13\pm 0.04$ Å was found.^{8,26} In those studies, owing to the absence of the higher shell contribution coming from the silver substrate, the XAS study alone was unable to define the NiO/Ag(001) interface and independent techniques have been employed; PDME data and *ab initio* simulations indicated an interface in which the O atoms are located on top of Ag atoms, as illustrated in the inset of Fig. 2. From this datum, and assuming a Ni-O distance at the interface layer equal to $1/2a_{\text{Ag}(001)}$, a value of $d=2.37\pm 0.05$ Å was inferred.^{8,26} The present study demonstrates the oxygen on top geometry and confirms the in-plane Ni-O distance. The XAS technique becomes therefore self consistent in the determination of the NiO/Ag(001) interface when the Ni K edge data are coupled with the O K edge ones. In the data

presented here, an O-Ag contribution at $r_{\text{O-Ag}} = 2.28 \pm 0.08 \text{ \AA}$ has been detected. Combining this result with previous ones ($r_{\text{Ni-Ag}} = 3.13 \pm 0.04 \text{ \AA}$), we conclude that the NiO films grow on Ag(001) in the O-on-Ag configuration (thus $d = r_{\text{O-Ag}}$; see the inset of Fig. 2), being both the Ni-on-Ag and the bridge site configurations incompatible with the two edges results. The picture obtained from experimental data agrees with a periodic *ab-initio* approach using the CRYSTAL code,⁸ where an O-on-top configuration was confirmed to be more stable than the Ni-on-top one by 0.25 eV/NiO unit and an interface distance of $d = 2.40 \text{ \AA}$ was computed (Table I).

By looking at the d values reported in Table I, values in the 2.28–2.40 \AA range are found; it is evident that we are dealing with a consistent expansion of the NiO/Ag(001) interface distance with respect to both the substrate half lattice parameter ($a_{\text{Ag(001)}}/2 = 2.045 \text{ \AA}$) and half that of the NiO film ($a/2 = 2.088 \text{ \AA}$). This effect seems to be a general feature, since a significant expansion has been observed for the MgO/Ag(001) system too,^{27–29,35} where a $d_{\text{MgO-Ag}} = 2.51 \pm 0.03 \text{ \AA}$, corresponding to a $(20 \pm 1)\%$ expansion with respect to half the bulk MgO interplanar distance ($a/2 = 2.110 \text{ \AA}$), has been found by polarization dependent XAS (Refs. 27 and 28) and has been confirmed by *ab initio* calculations.³⁵ The slightly larger expansion of MgO-Ag interplanar distance may be ascribed to the higher degree of ionicity of the Mg-O bond, compared to the Ni-O one, and thus to a reduced strength of O-Ag bonding at the MgO/Ag interface. In this regard, it is worth recalling that for the inverse system Ag deposited on MgO(100), Lagarde *et al.*^{36,37} have found an Ag-O distance $r_{\text{Ag-O}} = d = 2.53 \pm 0.05 \text{ \AA}$ by means of EXAFS at the Ag K edge in the 1–3 ML range. Even if the growth procedure is different in the two cases, i.e. a (1×1) structure in the NiO/Ag(001) and MgO/Ag(001) cases vs structurally coherent Ag islands in the case of Ag/MgO(100), the interface distance assumes comparable values in the two systems.

Before entering in the discussion of the Debye-Waller factors reported in Table II, some comments related to the adopted fitting strategy have to be discussed. Owing to the much shorter k -range available for this O K edge study (up to 8 \AA^{-1}) the number of independent points in data ($2\Delta k \Delta r / \pi$)

lies in the 10.10–10.96 range (see Table II) and additional constraints must be applied in the fitting procedures with respect to those adopted in the Ni K edge study, where analyzable signals up to 13 \AA^{-1} have been acquired.^{8,25,26} We therefore fixed the coordination numbers to those expected in the case of a perfect two-dimensional layer: e.g., 4 in-plane Ni first shell neighbors for any T and $2(T-1)/T$ out-of-plane Ni first shell neighbors for an epilayer of T ML. The same holds for higher shells contributions. This is of course, a non-negligible approximation (particularly for low T values). In fact, we know that the growth is not perfectly two-dimensional, as some islands of the $(n+1)$ layer start growing before the growth of the n layer has been totally accomplished. This results in surface O atoms in a lower coordination environment such as those located on corners or on steps.^{38,39} All these deviations from perfect two-dimensional growth are empirically taken into account in the optimized Debye-Waller factors which results thus overestimated with respect to what expected on the basis of the pure vibrational contribution, to take into account the reduction of the EXAFS signal caused by O atoms in defective surface positions. A progressive increase of the first shell Debye-Waller factor is systematically observed with increasing the expected sample defectivity (see Table II from top to bottom), where σ_1^2 moves from 0.003 to 0.016 \AA^2 when going from the 50 ML sample to the 3 ML sample measured in p -polarization. The second and third shells Debye-Waller factors exhibit mean values comparable with the corresponding uncertainty and have therefore not been reported in Table II as they are not reliable. They just played the role of adjustable phenomenological parameters which optimized values have to take into account for the simplicity of the adopted model: perfect two-dimensional NiO films.

ACKNOWLEDGMENTS

This work has been funded by INFN under PRA-ISADORA; measurements at ELETTRA were partially supported by the INFN Synchrotron Radiation Committee. We are indebted to the staff of the ALOISA beamline of the ELETTRA facility (in particular to A. Morgante, A. Cossaro and L. Floreano) for excellent support during the XAS measurements.

*Electronic address: carlo.lamberti@unito.it

¹Y. T. Matulevich, T. J. Vink, and P. A. Z. van Emmichoven, *Phys. Rev. Lett.* **89**, 167601 (2002).

²Hans-Joachim Freund, *Adsorption of Gases on Complex Solid Surfaces (Angewandte Chemie International)*, Eng. ed. (1997), Vol. 36, pp. 452–475, <http://www3.interscience.wiley.com/cgi-bin/jhome/26737>

³D. A. Muller, D. A. Shashkov, R. Benedek, L. H. Yang, J. Silcox, and D. N. Seidman, *Phys. Rev. Lett.* **80**, 4741 (1998).

⁴H. L. Meyerheim, R. Popescu, J. Kirschner, N. Jedrecy, M. Sauvage-Simkin, B. Heinrich, and R. Pinchaux, *Phys. Rev. Lett.* **87**, 076102 (2001).

⁵S. Schintke, S. Messerli, M. Pivetta, F. Patthey, L. Libioulle, M. Stengel, A. De Vita, and W. D. Schneider, *Phys. Rev. Lett.* **87**, 276801 (2001).

⁶S. A. Chambers, *Surf. Sci. Rep.* **39**, 105 (2000).

⁷D. W. Goodman, *J. Vac. Sci. Technol. A* **14**, 1526 (1996).

⁸C. Lamberti, E. Groppo, C. Prestipino, S. Casassa, A. M. Ferrari, C. Pisani, C. Giovanardi, P. Luches, S. Valeri, and F. Boscherini, *Phys. Rev. Lett.* **91**, 046101 (2003).

⁹K. Marre, H. Neddermeyer, A. Chasse, and P. Rennert, *Surf. Sci.* **358**, 233 (1996).

¹⁰P. Luches, S. Altieri, C. Giovanardi, T. S. Moia, S. Valeri, F. Bruno, L. Floreano, A. Morgante, A. Santaniello, A. Verdini, R.

- Gotter, and T. Hibma, *Thin Solid Films* **400**, 139 (2001).
- ¹¹C. Giovanardi, A. di Bona, S. Altieri, P. Luches, M. Liberati, F. Rossi, and S. Valeri, *Thin Solid Films* **428**, 195 (2003).
- ¹²F. Muller, R. de Masi, P. Steiner, D. Reinicke, M. Stadtfeld, and S. Hufner, *Surf. Sci.* **459**, 161 (2000).
- ¹³J. Wollschlager, D. Erdos, H. Goldbach, R. Hopken, and K. M. Schroder, *Thin Solid Films* **400**, 1 (2001).
- ¹⁴M. Schulze and R. Reissner, *Surf. Sci.* **507**, 851 (2002).
- ¹⁵M. Portalupi, L. Duo, G. Isella, R. Bertacco, M. Marcon, and F. Ciccacci, *Phys. Rev. B* **64**, 165402 (2001).
- ¹⁶R. Reissner, U. Radke, M. Schulze, and E. Umbach, *Surf. Sci.* **402**, 71 (1998).
- ¹⁷R. Reissner and M. Schulze, *Surf. Sci.* **454**, 183 (2000).
- ¹⁸I. Sebastian, T. Bertrams, K. Meinel, and H. Neddermeyer, *Faraday Discuss.* **114**, 129 (1999).
- ¹⁹T. Bertrams and H. Neddermeyer, *J. Vac. Sci. Technol. B* **14**, 1141 (1996).
- ²⁰D. Spanke, V. Solinus, D. Knabben, F. U. Hillebrecht, F. Ciccacci, L. Gregoratti, and M. Marsi, *Phys. Rev. B* **58**, 5201 (1998).
- ²¹D. Alders, L. H. Tjeng, F. C. Voogt, T. Hibma, G. A. Sawatzky, C. T. Chen, J. Vogel, M. Sacchi, and S. Iacobucci, *Phys. Rev. B* **57**, 11623 (1998).
- ²²S. Casassa, A. M. Ferrari, M. Busso, and C. Pisani, *J. Phys. Chem. B* **106**, 12978 (2002).
- ²³S. Altieri, M. Finazzi, H. H. Hsieh, H. J. Lin, C. T. Chen, T. Hibma, S. Valeri, and G. A. Sawatzky, *Phys. Rev. Lett.* **91**, 137201 (2003).
- ²⁴R. Dovesi, R. Orlando, C. Roetti, C. Pisani, and V. R. Saunders, *Phys. Status Solidi B* **217**, 63 (2000).
- ²⁵P. Luches, E. Groppo, C. Prestipino, C. Lamberti, C. Giovanardi, and F. Boscherini, *Nucl. Instrum. Methods Phys. Res. B* **200**, 371 (2003).
- ²⁶E. Groppo, C. Prestipino, C. Lamberti, P. Luches, C. Giovanardi, and F. Boscherini, *J. Phys. Chem. B* **107**, 4597 (2003).
- ²⁷P. Luches, S. D'Addato, S. Valeri, E. Groppo, C. Prestipino, C. Lamberti, and F. Boscherini, *Phys. Rev. B* **69**, 045412 (2004).
- ²⁸P. Luches, E. Groppo, S. D'Addato, C. Lamberti, C. Prestipino, S. Valeri, and F. Boscherini, *Surf. Sci.* **566–568**, 84 (2004).
- ²⁹C. Lamberti, *Surf. Sci. Rep.* **53**, 1 (2004).
- ³⁰L. Floreano, G. Naletto, D. Cvetko, R. Gotter, M. Malvezzi, L. Marassi, A. Morgante, A. Santaniello, A. Verdini, F. Tommasini, and G. Tondello, *Rev. Sci. Instrum.* **70**, 3855 (1999).
- ³¹A. L. Ankudinov, B. Ravel, J. J. Rehr, and S. D. Conradson, *Phys. Rev. B* **58**, 7565 (1998).
- ³²D. Alders, F. C. Voogt, T. Hibma, and G. A. Sawatzky, *Phys. Rev. B* **54**, 7716 (1996).
- ³³M. Newville, *J. Synchrotron Radiat.* **8**, 96 (2001).
- ³⁴J. F. Wang, E. F. Fisher, and M. H. Manghnazmi, *Chin. Phys. Lett.* **8**, 153 (1991).
- ³⁵C. Giovanardi, A. Di Bona, T. S. Moia, S. Valeri, C. Pisani, M. Sgroi, and M. Busso, *Surf. Sci.* **505**, L209 (2002).
- ³⁶P. Lagarde, S. Colonna, A. M. Flank, and J. Jupille, *Surf. Sci.* **524**, 102 (2003).
- ³⁷A. M. Flank, R. Delaunay, P. Lagarde, M. Pompa, and J. Jupille, *Phys. Rev. B* **53**, R1737 (1996).
- ³⁸A. Zecchina, D. Scarano, S. Bordiga, G. Spoto, and C. Lamberti, *Adv. Catal.* **46**, 265 (2001).
- ³⁹G. Spoto, E. Gribov, G. Ricchiardi, A. Damin, D. Scarano, S. Bordiga, C. Lamberti, and A. Zecchina, *Prog. Surf. Sci.* **76**, 71 (2004).